STRUCTURAL CHARACTERISATION OF DEFECTS IN CFRP LAMINATES PRODUCED WITH DIFFERENT EPOXY RESIN SYSTEMS AND THEIR INFLUENCE ON THE MECHANICAL PROPERTIES

M. Rodríguez-Hortalá[1*], J. Hatzmann[1, 2], H. P. Degischer[1]

[1]*Institute of Materials Science and Technology, Vienna University of Technology, Karlsplatz 13/E308 – A-1040 Vienna, Austria*
[2]*LIST components & furniture GmbH, List-Straße 1 – A-2842 Edlitz-Thomasberg, Austria*
**mrodrig@mail.tuwien.ac.at*

Keywords: CFRP laminates, porosity, computed tomography, bending test

Abstract
The studied materials are CFRP laminates produced by hand layup using the same carbon fabric and two different epoxy systems. The composites architecture was analyzed (light microscopy (LOM), scanning electron microscopy (SEM) and computed tomography) to identify and characterize existing defects within the microstructure of the samples. Furthermore the mechanical parameters were determined by bending and short beam shear tests. The glass transition temperature was studied using DMA (Dynamic Mechanical Analysis) and DSC (Differential Scanning Calorimetry). Thermogravimetrical analysis (TGA) was conducted to estimate fibre volume fraction and porosity content. SEM fractography analysis of bending and samples after mechanical testing was used to study failure modes and correlate the observed features with the previously detected defects and the variation of the mechanical and thermal properties originated by their presence.

1 Introduction
Because of their high stiffness and strength in combination with low weight, fibre reinforced polymers (FRP) are used commonly. Though design, dimensioning and manufacturing of such structures varies a lot compared to monolithic light weight materials like aluminium alloys [1]. Whilst dimensioning using finite element methods is nowadays grown-up methodology, the correlation between defects, which are always inherent in composite structures and their effect on the types of failure of fibre composite components is not yet fully understood. Carbon fibre reinforced polymer (CFRP) composites are manufactured mainly by hand layup. Epoxy resin is most often used as matrix material. The mechanical properties are directly influenced by the constitution, the fibre volume fraction and the porosity of the material. The fibre-matrix interface properties (which depend on one hand on the actual components and on the other hand on the way the composite is manufactured) are also of critical importance. The aim of this work is to study quantitatively and qualitatively the relationships between microstructure (in particular defects) and material properties by using a combination of different methods, which allow us having complementary perspectives of the studied phenomena. Furthermore a comparison of two different matrix systems and their influence on the mechanical performance of the composites is intended as well.

2 Materials and experimental methods

2.1 Materials: CFRP laminates

Carbon fibre reinforced polymer (CFRP) laminates produced by hand lay-up were studied. The reinforcement being continuous carbon fibre textiles and the matrix an epoxy resin.

Two series of composite materials were produced using the same carbon textiles and two different epoxy resin systems to study the influence of the matrix on the composite properties. Table 1 shows an overview of the studied materials and the abbreviations used in this work.

No.	Code	Epoxy Matrix	C-Fibres	Carbon textile	Curing-method
1	Ep-Sik/C-FT300/0-90°/1bar	Sika Biresin CR132	Torayca Carbon FT 300B	0°/90° CF-fabric	vacuum-bag moulding: 1bar post-curing: 8h-120°C
2	Ep-Sik/C-HTA40/UD/1bar	Sika Biresin CR132	Toho Tenax Carbon HTA 40	UD fabric: 95% CF 0° 05% GF 90°	
3	Ep-Sik/C-HTS5631/UD/1bar	Sika Biresin CR132	Toho Tenax Carbon HTS 5631	UD CF-band + PES Fibre	
4	Ep-Sik/C-HTS5631/UD/3bar	Sika Biresin CR132	Toho Tenax Carbon HTS 5631	UD CF-band + PES-Fibre	pressurized chamber: 3bar post-curing: 8h-120°C
5	Ep-Hex/C-FT300/0-90°/1bar	Hexion L418	Torayca Carbon FT 300B	0°/90° CF-fabric	vacuum-bag moulding: 1bar post-curing: 15h-140°C
6	Ep-Hex/C-HTA40/UD/1bar	Hexion L418	Toho Tenax Carbon HTA 40	UD fabric: 95% CF 0° 05% GF 90°	
7	Ep-Hex/C-HTS5631/UD/1bar	Hexion L418	Toho Tenax Carbon HTS 5631	UD CF-band + PES-Fibre	
8	Ep-Hex/C-HTS5631/UD/3bar	Hexion L418	Toho Tenax Carbon HTS 5631	UD CF-band + PES-Fibre	pressurized chamber: 3bar post-curing: 15h-140°C

Table 1. Studied composite materials. 1-4 produced with Sika Biresin CR132 epoxy system, 5-8 with Hexion L418 system.

Two types of epoxy resin (Sika CR132 and Hexion L418) were combined with three types of carbon fibres. The selected matrix materials are particularly suitable for hand lay-up and have a high temperature resistance. Regarding C-fibre arrangement we can distinguish between materials 1 and 5 (0°/90°) and the rest materials (UD). Materials 1-3 and 5-7 were cured in a vacuum bag at 1 bar, whilst 4 and 8 materials under 3 bar in a pressurized chamber. Post-curing was done afterwards at different conditions depending on the matrix system. Table 2 shows the main properties of the matrix material at a glance.

Property	Biresin CR 132	Laminating resin L418
Manufacturer	Sika	Hexion
Tensile strength	78 MPa	75-90 MPa
E-Modulus	2,7 GPa	3,3-3,6 GPa
Ultimate strain	5,7 %	5-6 %
Density	1.14* g/cm³	1,15 g/cm³
Glass transition temperature	135 °C	120-125 °C

Table 2. Properties of the studied matrix systems, from [2] and [3]. *)This value was experimentally determined.

2.2 Experimental methods

Light optical microscopy (LOM) as well as x-ray computed tomography (XCT) were used for structural characterisation and to assess manufacturing defects present in each composite.
TGA, DSC, DMA, bending tests, SBS test, and post mortem SEM fractography were carried out to study the influence of the different matrix system and of the found production defects on the composites thermal and mechanical properties.

2.2.1 Materialography

2.2.1.1 LOM (light optical microscopy)

Optical micrographs were made on a Zeiss Axioplan microscope. All samples were embedded in an Araladit® epoxy cylinder and subsequently ground and polished at a Struers Tegra Doser-5 machine.

2.2.1.2 Computed X-ray tomography (XCT)

XCT Scans were performed using a sub-µm-CT device Nanotom (GE Phoenix|x-ray, Wunstorf, Germany). The resolution results from the size of the specimens that were prepared and from the volume analyzed, a voxel size = $(16\ \mu m)^3$ was used for the studied laminates. Only samples 4 and 8 (cured under 3 bar) were studied with this technique.

2.2.2 Thermogravimetric analysis (TGA)

TGA was carried out using a TA-Instruments TGA 2050 device. Sample weigh was about 150 mg. TGA analysis was carried out using a neutral nitrogen atmosphere from 25°C to 850°C. The heating rate was 10°C/min.

2.2.3 Differential scanning calorimetry (DSC)

The system used was a TA Q2000 Calorimeter from TA Instruments, which offers the possibility of modulated measurements (MDSC). Thus, the heat flow can be separated into a reversible and a non reversible part facilitating the evaluation as the step defining the glass transition temperature is more distinct in case of the reversible heat flow curve. Specimen weight was around 30 mg. Slices were cut out using a circular saw and were grinded manually to be encapsulated in standard aluminium pans. Measurements took place between 30°-250°C with a heating rate of 3°C/min and temperature modulation ± 1°C/min.

2.2.4 Dynamic mechanical analysis (DMA)

The test method used was a three point bending test on a TA Instruments 2980 dynamic mechanical analyzer. Sample length is 60 mm, the support distance 50 mm, the width and height of the samples are selected not to exceed the maximum force of 15 N. The amplitude of the deformation 70 µm, the loading frequency 1 Hz. Storage modulus, loss modulus and loss factor were recorded between 25° and 200°C with a heating rate of 3°C/min.

2.2.5 Bending test

Flexural properties of the laminates were determined by four point bending test according to the EN ISO 14125 standard [4] on a universal testing machine Zwick H050 with a 50 kN load cell. Sample dimensions and clamping length is chosen to fit earlier tests carried out but the same manufacturer with the same fibres and fabrics, but other resins. Specimens were loaded at a speed of 5 mm/min with a lower span of 190 mm and an upper span of 50 mm. The radius of the supports (movable rollers) was 5 mm. Deflection and force are recorded during the test and converted into flexural strain-stress curves taking the geometry of the samples and the span lengths into account.

2.2.6 Short beam shear test (SBS)
SBS tests were carried out to determine the interlaminar in accordance with the ASTM D2344 standard [5] on a universal testing machine Zwick H050 with a 50 kN load cell. The set-up is like a three point bending test, being the samples much shorter. Specimens were loaded at a speed of 1 mm/min with a lower span between 16-24 mm depending on the sample. Afterwards the interlaminar shear strength is calculated from the maximum force values.

2.2.7 SEM fractography
Scanning electron images were made in a Philips XL 30 SE microscope at 15kV, samples were first made electrically conductive by coating them with an extremely thin layer of gold in an Agar Sputter Coater machine. For interpretation of fractographic features typical of fibre reinforced polymers [6] was consulted.

3 Results

3.1 Materialography

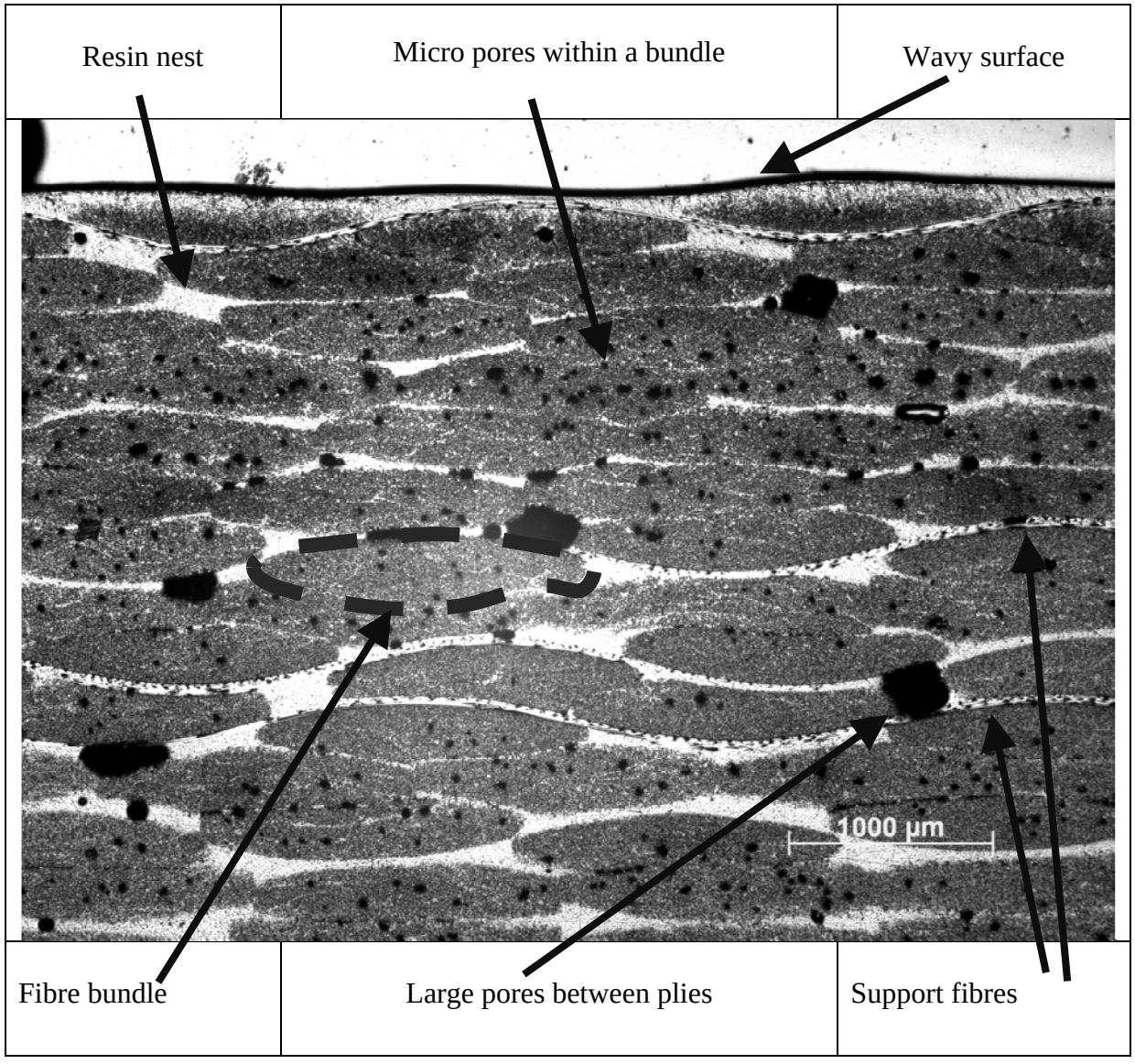

Figure 1. Cross section LOM micrograph of Sik/C-HTA40/UD/1 bar material. Observed defects are indicated.

During manual lay-up, air bubbles are introduced between the layers which in spite of the pressure applied while curing result in some reminiscent macro and micro porosity.
Typical defects for the studied materials observed in LOM micrographs are: two kinds of porosity, micro pores within a bundle, macro porosity (voids) between plies, longitudinal tunnel-like porosity, shrinkage porosity, fibre waviness, misaligned fibres, broken fibres, unimpregnated areas close to the surface, textile transition edges, matrix rich areas between plies as well as different fibre packing densities within bundles. Some of these defects can be observed in Figures 1 and 2. For more micrographs of all eight different materials see [7].

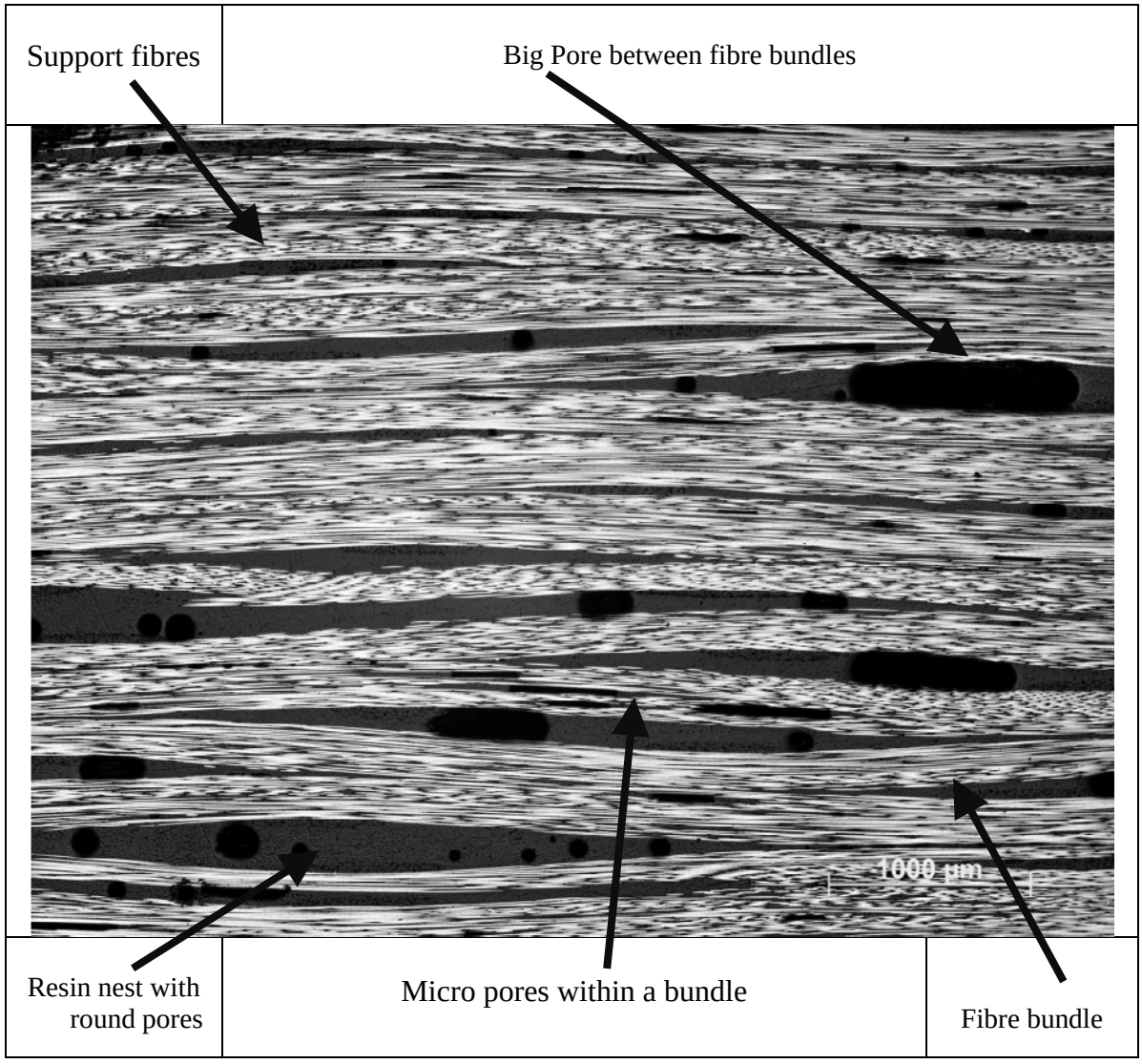

Figure 2. Longitudinal section LOM micrograph of Sik/C-HTA40/UD/1 bar material with observed defects.

Porosity volume fraction was determined from XCT measurements for the samples cured under 3 bar pressure. The pores appear as darker areas, i.e. with lower grey values. Segmentation was carried out applying a global grey value threshold. Objects smaller than 27 voxels were disregarded. The textile in these composites has additionally to the C-fibres some PES support fibres perpendicular to the C-fibre bundles. A 3D view of segmented porosity is shown in Figure 3. The largest porosity accumulations are oriented in the direction of the support fibres, whereas smaller porosity channels run in C-fibre direction. Between plies very large pores (from air bubbles introduced during manual lay-up) are easily recognized. The distribution of the porosity within the material is relatively homogenous.

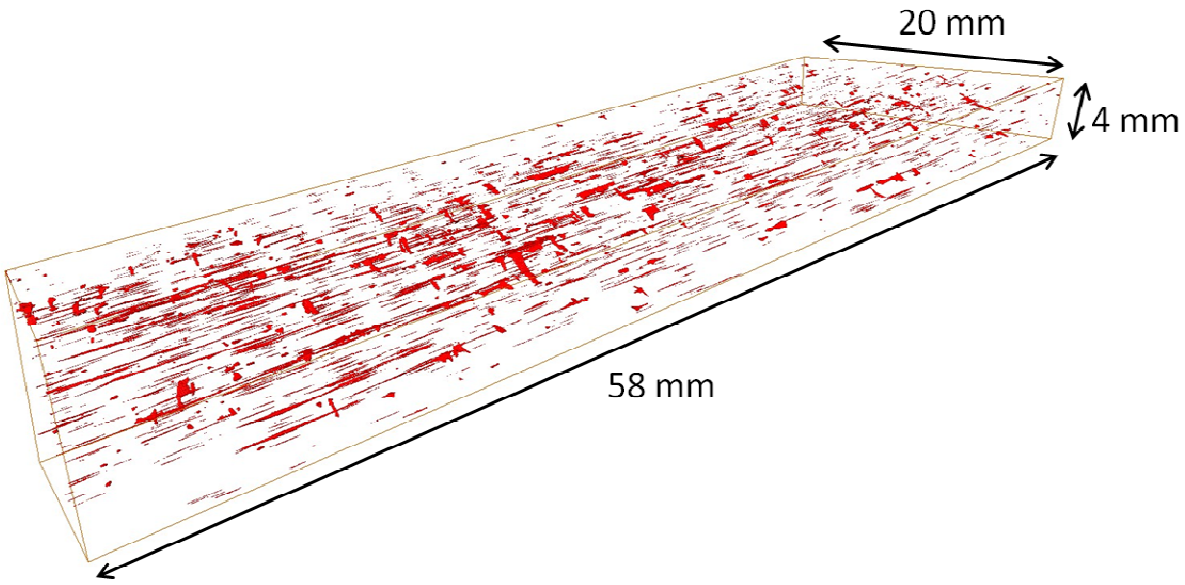

Figure 3. 3D view of segmented porosity within a 4640 mm^3 volume of sample Sik/C-HTS5631/UD/3bar.

3.2 TGA

Pure resin and fibres samples were analyzed separately. It was found that at 600°C, 96% of the resin and only 2% of the fibres were vaporized. Mass fractions were recalculated taking this into account (Table 3). Degradation of the epoxy resin takes places between 350-550°C. No degradation of the carbon fibres occurs because of the non-oxidative nitrogen atmosphere.

Material	**W_f %**	**W_m %**	**V_f %**	**V_m %**	**$V_{porosity}$ %**	**XCT $V_{porosity}$ %**
1	55.9	44.1	43.8	52.9	3.3	-
2	65.9	34.1	53.9	43.0	3.0	-
3	68.8	31.2	57.2	40.2	2.6	-
4	73.3	26.7	63.8	36.0	**0.2**	**0.2**
5	66.6	33.4	53.6	41.0	5.4	-
6	71.6	28.4	57.8	35.1	7.2	-
7	77.6	22.4	62.7	27.9	9.5	-
8	76.0	24.0	65.7	31.9	**2.4**	**2.5**

Table 3. Obtained mass and volume faction of the components and porosity volume fraction. For samples 4 and 8 porosity volume fraction values obtained from XCT are included in the table for comparison with TGA ones.

3.3 Thermal analysis

3.3.1 DSC + DMA

Material	**DSC**			**<Tg (°C)>**	**DMA**	
	$T_{g\ Beginning}$ (°C)	**T_g (°C)**	**$T_{g\ End}$ (°C)**		**E' (GPa)**	**T_g (°C)**
1	116	125 ± 4	129	DSC	34.8	119 ± 3
2	105	117 ± 0	126	127 ± 5	91.2	121 ± 1
3	122	129 ± 0	136	DMA	100.8	124 ± 2
4	124	129 ± 1	133	122 ± 3	106.5	124 ± 2
5	112	119 ± 2	124	DSC	52.2	125 ± 1
6	108	115 ± 1	121	111 ± 6	88.3	125 ± 0
7	98	105 ± 3	110	DMA	113.6	123 ± 1
8	100	107 ± 2	113	124 ± 1	116.8	122 ± 0

Table 4. Glass transition temperature (T_g) intervals obtained from DSC curves, indicating beginning and end of the endothermic transition step. Storage E-Modulus and T_g obtained from DMA curves. Since the Tg is a matrix property an average <T_g> was calculated for each studied epoxy system and each method.

3.4 Mechanical characterisation

3.4.1 Four point bending test

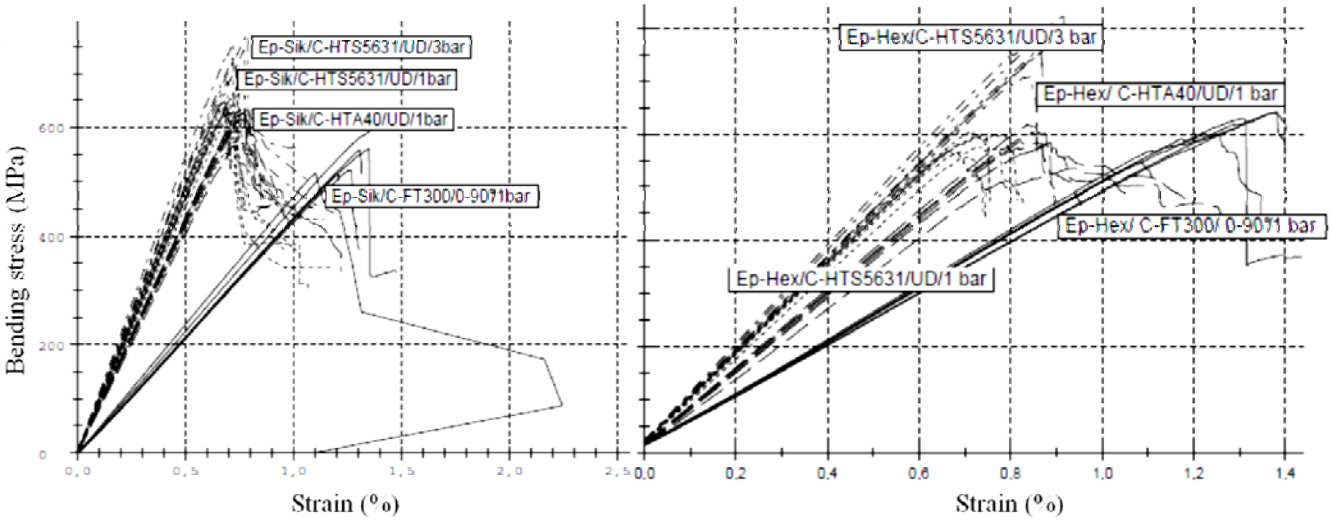

Figure 4. Stress-strain diagrams for samples produced with Sika (left) and Hexion matrix (right).

3.4.2 SBS

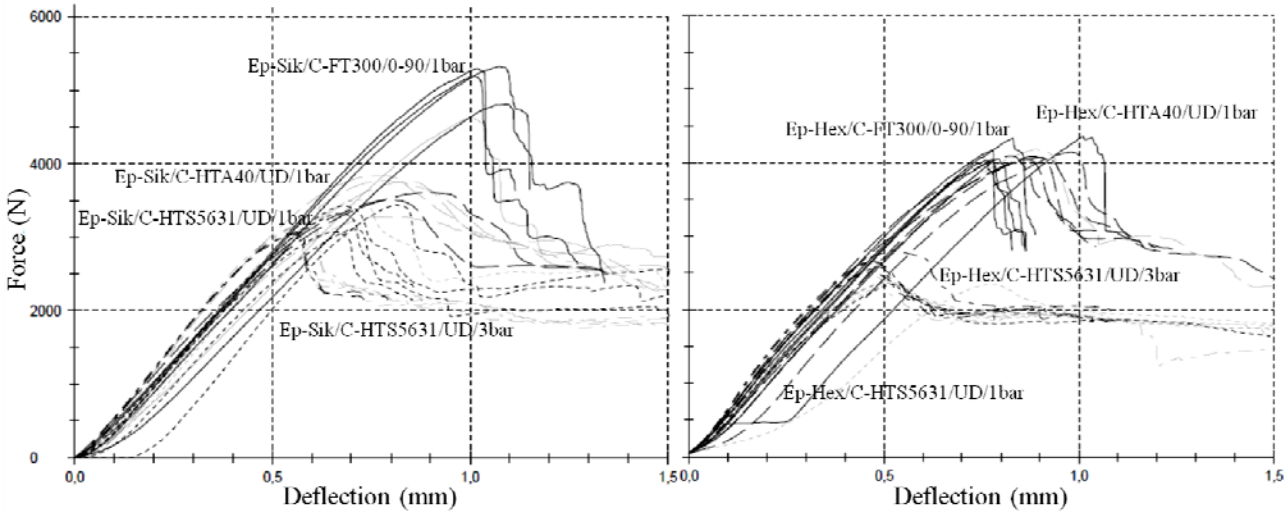

Figure 5. SBS results for samples produced with Sika (left) and Hexion matrix (right).

Material	4-Point Beinding Test			Short Beam Shear		$V_{porosity}$
	E_b (GPa)	σ_b (MPa)	ε_b (%)	F_{max} (N)	F^{sbs} (MPa)	%
1	43 ± 3	544 ± 33	1.27 ± 0.10	5045 ± 311	54.4 ± 3.3	3.3
2	85 ± 2	616 ± 23	0.76 ± 0.02	3625 ± 208	51.1 ± 1.4	3.0
3	93 ± 3	628 ±13	0.69 ± 0.03	3312 ± 181	53.1 ± 0.9	2.6
4	102 ± 6	725 ± 42	0.74 ± 0.03	3118 ± 74	61.7 ± 1.4	0.2
5	48 ± 1	544 ±93	1.32 ± 0.12	4161 ± 153	53.0 ± 1.1	5.4
6	70 ± 3	468 ± 23	1.05 ± 0.17	4103 ± 51	55.9 ± 1.1	7.2
7	83 ± 2	461 ± 15	0.77 ± 0.04	2361 ± 18	39.6 ± 0.5	9.5
8	88 ± 3	725 ± 94	0.88 ± 0.02	2617 ± 111	53.0 ± 2.2	2.4

Table 5. Average results of the mechanical tests carried out. The shear strength in Hexion samples is smaller.

It was observed that high porosity volume fractions, especially above 5% have a detrimental influence on both stiffness (E_b) and strength (σ_b) of the laminates. Interlaminar shear strength results reveal that the fibre-matrix adhesion of Hexion-based composite materials is poorer than for their Sika counterparts.

3.5 SEM fractography

Figure 6 shows compression and tension failure of the plies and delamination, a very critical issue for CFRP laminates. Figure 7 shows fractography images of a delaminated surface.

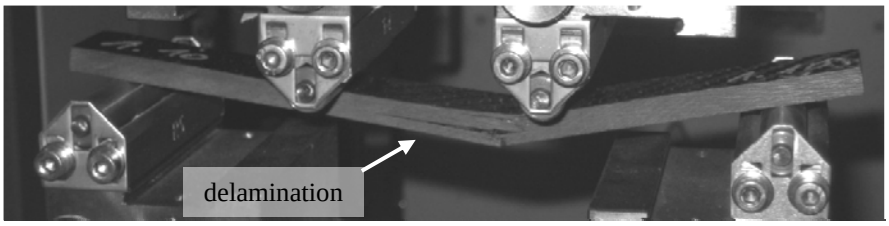

Figure 6. Failure behaviour of a laminate during 4-point bending test observed on the macroscopic scale.

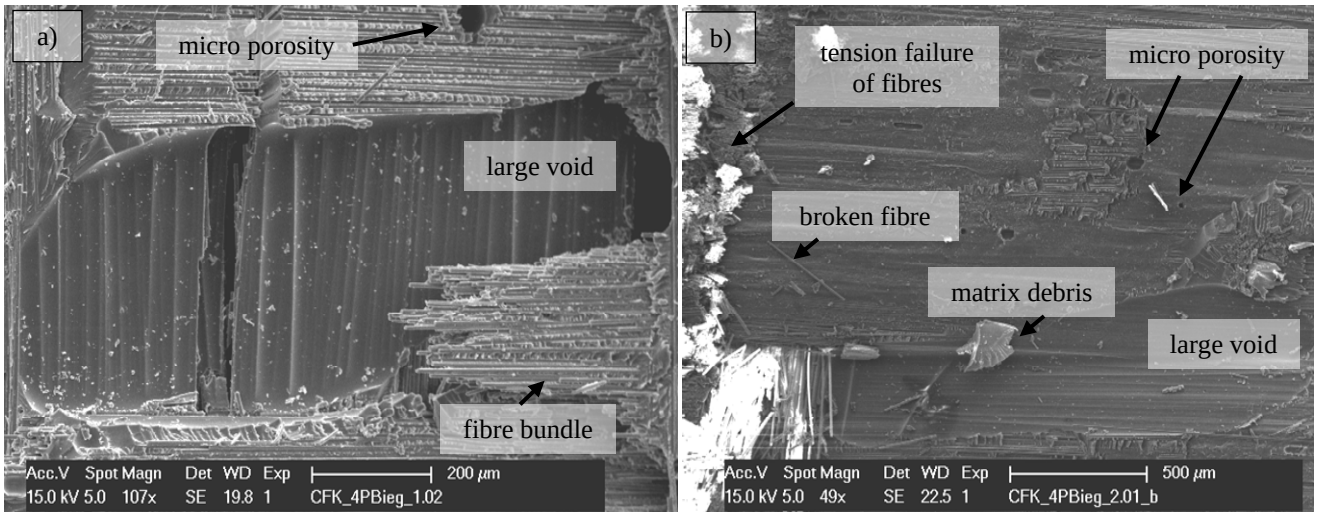

Figure 7. SEM fractographies of a sample after 4-point bending test. a) Large void 1mmx0.5mm on a delaminated surface. b) Typical fractographic features: bare fibres, matrix debris, macro and micro porosity.

4 Conclusions

Effect of defects: Pore (void) size and porosity volume fraction are considerably higher in laminates cured at 1 bar (Table 3), as well as the amount of touching fibres observed. The natural waviness of the C- fibres within a ply results in many contact points between adjacent fibres [7]. Most of the defects observed in the laminates are between plies, as a consequence of the manufacturing process. Hexion resin system appears to be less manufacture-friendly yielding higher porosity volume fraction for all four composites (Table 3), with the consequent decrease of the mechanical properties E_b and σ_b (Table 5) although the fibre volume fraction is higher for the composites produced with this resin (Table 3). This confirms the relationship between damage and higher porosity values. Delamination between plies is more likely to take place if big pores or resin nest (with the consequent decrease of reinforcement volume fraction) are present. Support PES fibres associated to large pores perpendicular to the carbon bundles, also deteriorate properties.

References

[1] Ehrenstein G. W. *Faserverbund-Kunststoffe*. München: Carl Hanser. 2006.
[2] HEXION. Technical Information Laminating resin MGS L418. Stuttgart. 2006.
[3] Sika Produktdatenblatt Biresin CR132. Compositeharz-System. 2010.
[4] EN ISO 14125. 1998.
[5] ASTM D2344. 2000.
[6] Greenhalgh E. S. *Failure analysis and fractography of polymer composites*. Woodhead Publishing Limited and CRC Press LLC. 2009.
[7] Hatzmann J. *Identifizierung von Fehlstellen in Karbonfase Epoxidharz Laminaten und Vergleich zweier Harzsysteme, sowie deren Einfluss auf die mechanischen Eigenschaften.* Master Thesis. TU Wien. 2011.